Accessing Extreme Spatiotemporal Localization of High-Power Laser Radiation through Transformation Optics and Scalar Wave Equations

V. Yu. Fedorov,[1,2,*] M. Chanal,[3] D. Grojo,[3] and S. Tzortzakis[1,4,5,†]
[1]Science Program, Texas A&M University at Qatar, P.O. Box 23874 Doha, Qatar
[2]P. N. Lebedev Physical Institute of the Russian Academy of Sciences, 53 Leninskiy Prospekt, 119991 Moscow, Russia
[3]Aix Marseille University, CNRS, LP3, F-13288 Marseille, France
[4]Institute of Electronic Structure and Laser (IESL), Foundation for Research and Technology—Hellas (FORTH), P.O. Box 1527, GR-71110 Heraklion, Greece
[5]Materials Science and Technology Department, University of Crete, 71003 Heraklion, Greece
(Received 16 March 2016; published 22 July 2016)

Although tightly focused intense ultrashort laser pulses are used in many applications from nanoprocessing to warm dense matter physics, their nonparaxial propagation implies the use of numerical simulations with vectorial wave equations or exact Maxwell solvers that have serious limitations and thus have hindered progress in this important field up to now. Here we present an elegant and robust solution that allows one to map the problem on one that can be addressed by simple scalar wave equations. The solution is based on a transformation optics approach and its validity is demonstrated in both the linear and the nonlinear regime. Our solution allows accessing challenging problems of extreme spatiotemporal localization of high power laser radiation that remain almost unexplored theoretically until now.

DOI: 10.1103/PhysRevLett.117.043902

Introduction.—Tightly focused ultrashort laser pulses are used in many applications including laser machining of materials [1,2], eye surgery [3], and nanoprocessing of biological cells [4]. Also, the high intensities that can be achieved under such conditions enable warm dense matter studies and the observation of exciting new material states [5,6]. The interaction of tightly focused light with matter is strongly nonlinear and includes effects like self-focusing, multiphoton absorption, and plasma generation. Experimental studies of these complex propagation dynamics in such small volumes become extremely hard and therefore corresponding numerical simulations are necessary to elucidate the underlying physics.

Simulations of nonlinear propagation of ultrashort laser pulses in the case of collimated or loosely focused laser beams can be addressed by considering a scalar wave equation only for a single component of the laser field. However, in the case of tight focusing, the nonparaxial nature of the problem imposes the need to use a vectorial wave equation, that is, a separate equation for each component of the field, or the use of exact Maxwell solvers [7]. Both solutions suffer from the need of unrealistic large computational resources and time, and thus studies in the field of tightly focused ultrashort laser pulses in nonlinear media have been very limited until now.

There is only a small number of publications where the authors study nonlinear propagation of ultrashort laser pulses taking into account vectorial and nonparaxial effects [8–12]. Among them the majority considers these effects only as a mechanism that arrests the catastrophic intensity growth during the self-focusing [8,9,11]. As far as we know, only the papers by Arnold *et al.* [10] and Couairon *et al.* [12] are devoted specifically to simulations of tightly focused ultrashort pulses in nonlinear media. In both papers the authors develop appropriate vectorial wave equations. Finally, Ref. [12] demonstrated that tight focusing can, under conditions, be simulated using a scalar wave equation, though this solution cannot be applied to extreme focusing geometries.

Here we propose a simple and elegant solution where one maps the nonparaxial original problem on an equivalent problem of propagation in a medium with a higher refractive index, where the propagation becomes paraxial. This is a holistic solution and allows one to simulate the tight focusing without restrictions on the beam shape, focusing geometry, and numerical aperture, while it can be applied to any of the existing scalar wave equations, both linear and nonlinear.

In the following, we present in detail the solution and demonstrate its validity by comparing with exact vectorial models and experiments, both in the linear and the nonlinear regime.

Transformation solution.—Without loss of generality, let us consider a light beam focused by an objective with numerical aperture NA given by

$$\mathrm{NA} = n \sin\theta = n\frac{a}{f}, \tag{1}$$

where n is the refractive index of the propagation medium, θ is the half-angle of the maximum cone of light that can exit the objective, a is the radius of the objective's aperture, and f is the focal distance (see Fig. 1). To simulate this problem with a scalar wave equation, we specify the initial field, with

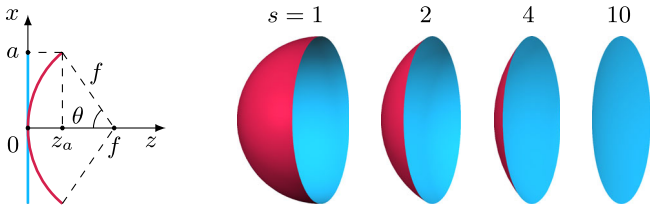

FIG. 1. Sketch of the transformation principle. The initial strongly curved wave front, responsible for the nonparaxial propagation effects, becomes flatter and approaches the paraxial propagation as one increases the scaling factor s.

a parabolic phase, in a plane perpendicular to the propagation direction (blue line in Fig. 1). Then, by successive iterations, we find the field in other transverse planes located further along the propagation axis. However, the field of a tightly focused beam after the objective is distributed on a curved surface (red line in Fig. 1) and the main source of inaccuracy in simulations of the tight focusing with scalar wave equations originates from the fact that one neglects the curvature of this surface [12]. The most straightforward solution to this problem would be to use the Maxwell equations, where we can specify the initial condition on an arbitrary surface by adding a longitudinal field component. However, Eq. (1) suggests another solution; namely, it tells us that in a medium with a higher refractive index n the same value of NA, that is, the same focusing tightness, can be obtained with smaller apertures or longer focal distances. Triggered by this observation and transformation optics analogies, we propose to map the original problem on a problem of propagation in a medium with a scaled refractive index n_s given by

$$n_s = sn, \tag{2}$$

where n is the original refractive index and s is a scaling factor (for complex $n = n' + in''$ the transformation should be $n_s = sn' + in''/s$). According to the Fermat principle, this new problem will be equivalent to the original one if at the same time we scale down by the same amount the propagation length.

As one increases the refractive index n of the medium by s times, while keeping constant the objective's aperture a (for conservation of energy), the focal distance also increases by the same factor, which can be interpreted as a stretching of space along the z axis. In Fig. 1 we show graphically how the strong wave front curvature is reduced in response to this space stretching. Above a certain scaling factor s, the spherical surface will be flat enough and one can safely apply a scalar wave equation. In order to return to the original geometry the only thing that one needs to do is to compress the space along the z axis by s times.

To quantify the changes in the curvature, let us calculate the distance z_a between the edge of the spherical surface and the plane $z = 0$. From Fig. 1 $z_a = f(1 - \cos\theta)$ and applying Eq. (1) with $n_s = sn$, we obtain

$$z_a = a\frac{sn}{\mathrm{NA}}\left(1 - \sqrt{1 - \frac{\mathrm{NA}^2}{(sn)^2}}\right). \tag{3}$$

A scalar wave equation becomes inaccurate when z_a exceeds the confocal parameter [12], which would limit the validity of scalar simulations up to NA ≈ 0.2. However, let us consider a much stronger condition, namely, let us demand z_a to be of the order of the wavelength λ of the focused light. Setting $z_a = \lambda$ in Eq. (3) we find

$$s = \frac{\mathrm{NA}}{n}\frac{a^2 + \lambda^2}{2a\lambda}. \tag{4}$$

From Eq. (4) for NA $= 1$, $a = 1$ mm, and $\lambda = 800$ nm the scaling factor is $s = 625$. In the following we will use $s = 1000$ in order to be always above this limit.

Linear propagation.—To verify the validity of our solution let us consider the following scalar nonparaxial wave equation:

$$\frac{\partial \hat{E}}{\partial z} = ik_z\hat{E}, \tag{5}$$

where $\hat{E}(k_x, k_y, z)$ is the spatial spectrum of the field, $k_z = (k_0^2 - k_x^2 - k_y^2)^{1/2}$ is the propagation constant, k_x and k_y are the spatial frequencies, $k_0 = n_0\omega_0/c_0$ is the wave number, n_0 is the refractive index at the wave's frequency ω_0, and c_0 is the speed of light in vacuum. As initial condition for Eq. (5) we take a flattop beam that corresponds to a part of plane wave passed through the objective's aperture:

$$E(x, y, z = 0) = \Theta(a - r)\exp\left(-ik_0\frac{r^2}{2f}\right), \tag{6}$$

where $r = (x^2 + y^2)^{1/2}$ and Θ is the step function. For applying the transformation solution to Eqs. (5) and (6), we replace the original refractive index n_0 by the scaled one, $n_s = sn_0$, and in order to keep the same NA we decrease the ratio a/f by s times [see Eq. (1)], which is done by increasing the focal distance f by s times. The change in the refractive index also affects the wave number k_0, which becomes s times larger. Therefore, the initial condition (6) does not change, since it depends only on the ratio k_0/f. The most important change affects the propagation constant k_z, which now reads as $k_z = [(sk_0)^2 - k_x^2 - k_y^2]^{1/2}$. Since the aperture a is not changed, the spatial spectrum does not change either. Therefore, by stretching the wave number k_0, we actually reach a point where $(sk_0)^2 \gg k_x^2 + k_y^2$ and where we can safely apply the paraxial approximation for k_z, namely, $k_z \approx sk_0 - (k_x^2 + k_y^2)/2sk_0$.

Using the new propagation constant k_z, either in its original or paraxial form (the latter does not change the result), we simulate the propagation with Eqs. (5) and (6). In order to return to the original problem, we have two

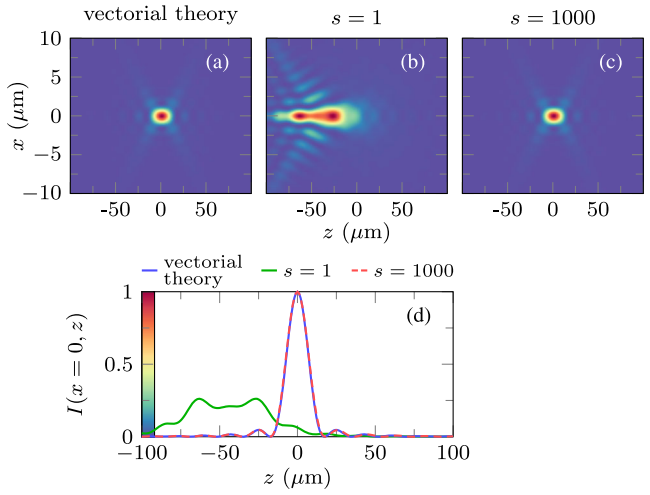

FIG. 2. Normalized intensity distributions of a plane wave focused by an objective with NA = 0.3. (a) Rigorous vectorial theory. (b) Scalar wave equation ($s = 1$). (c) Scalar wave equation with transformation ($s = 1000$). (d) Relative on-axis intensities. Focal position $f = 2$ mm corresponds to $z = 0$.

choices: we can either divide by s times the lengths along the propagation axis after the simulation, or we can use the original lengths, but increase by s times each step along the propagation axis.

To begin with, let us consider a plane wave with $\lambda_0 = 800$ nm focused by an objective with NA = 0.3 and aperture $a = 0.6$ mm into a medium with $n_0 = 1$. In this case, according to Eq. (1), the focal distance is $f = 2$ mm. Figure 2 depicts the normalized intensity distributions $I(x, z) = |E(x, y = 0, z)|^2$ near the focal zone. Figure 2(a) shows the result obtained by PSF Lab code that implements a rigorous vectorial theory developed by Nasse and Woehl [13]. Figure 2(b) shows the results of our simulations for $s = 1$ and Fig. 2(c) for $s = 1000$. Finally, Fig. 2(d) shows the relative on-axis intensities for all the above cases. One can clearly see that the intensity obtained in the simulation with $s = 1$ is strongly distorted and its peak intensity is considerably lower relative to the exact solution. On the contrary, the simulation with $s = 1000$ provides precisely the same solution as the exact vectorial theory.

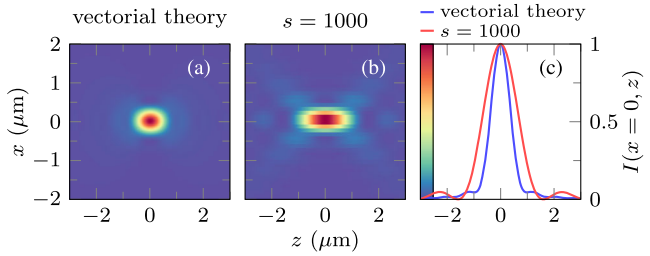

FIG. 3. Normalized intensity distributions of a plane wave focused by an objective with NA = 1. (a) Rigorous vectorial theory. (b) Scalar wave equation with $s = 1000$. (c) Normalized on-axis intensities. Focal position $f = 2$ mm corresponds to $z = 0$.

To verify the validity of our solution under extreme conditions we repeated the above simulations for NA = 1. Figure 3(a) shows the intensity profile near the focus from the exact vectorial theory, Fig. 3(b) shows the result of our simulation with $s = 1000$, and Fig. 3(c) compares the normalized on-axis intensities between the two. Again, one can clearly see that the transformation solution works surprisingly well: even in the extreme case of NA = 1 the difference between the simulated and the exact theory intensity distributions is less than 1 wavelength on the propagation direction, while on the transverse one they are exactly the same. The minor difference on the propagation axis appears because a small part of the beam energy goes into the longitudinal field component, which is neglected in scalar wave equations.

Nonlinear propagation.—In the previous section we demonstrated how the transformation solution can be applied for simulations of tightly focused monochromatic beams in linear media and show that the obtained results are in very good agreement with the rigorous vectorial theory. Since there is no exact theory that can be used to test the validity of the transformation approach for simulations of tightly focused ultrashort laser pulses in nonlinear media we will validate our solution by direct comparison with related nonlinear propagation experiments in silicon, a material exhibiting strong nonlinearities.

In our experiments we use a Ti:sapphire laser source combined with an optical parametric amplifier in order to generate 60 fs (FWHM) linearly polarized laser pulses at 1300 nm. Using microscope objectives of different NAs we tightly focus the generated laser pulses at the vicinity of the rear surface of a 1 mm pure crystalline silicon sample. We image the fluence distribution at the rear surface using a microscopy setup with an NA = 0.7 objective and an InGaAs camera. By moving the focusing objective along the optical axis, we obtain a stack of images that we use to reconstruct a full 3D fluence distribution of the beam around its focus. The details about our experimental technique can be found in Refs. [14,15].

For the simulations we use the scalar Unidirectional Pulse Propagation Equation [16] which corresponds to Eq. (5) with an additional nonlinear term:

$$\frac{\partial \hat{E}}{\partial z} = ik_z\hat{E} + i\frac{\mu_0\mu\omega^2}{2k_z}\left[\hat{P}_{nl} + \frac{i}{\omega}(\hat{J}_f + \hat{J}_a)\right], \qquad (7)$$

where $\hat{E} = \hat{E}(\omega, k_x, k_y, z)$ is the spatiotemporal spectrum of the laser pulse and the propagation constant is $k_z = [k^2(w) - k_x^2 - k_y^2]^{1/2}$. The nonlinear term in Eq. (7) includes the cubic nonlinear polarization, $\hat{P}_{nl} = (3/4)\varepsilon_0\chi^3|\hat{E}|^2\hat{E}$, the current of free electrons, $\hat{J}_f = (q_e^2/m_e)(\nu_c + i\omega)/(\nu_c^2 + \omega^2)\hat{\rho}\hat{E}$, and the current that is

responsible for multiphoton absorption, $\hat{J}_a = K\hbar\omega_0 \widehat{\frac{\partial\rho}{\partial t}\frac{1}{E}}$, where the caret denotes the spatiotemporal spectrum, ε_0 is the vacuum permittivity, $\chi^3 = 4n_0^2\varepsilon_0 c_0 n_2/3$ is the cubic susceptibility with $n_2 = 1.5 \times 10^{-18}$ m^2/W being the nonlinear index [17], q_e and m_e are the charge and mass of the electron, $\nu_c = 0.3 \times 10^{15}$ s^{-1} is the collisions frequency [18], ρ is the concentration of free electrons (in $1/\text{m}^3$), and $K = 2$ is the order of the multiphoton absorption. Together with Eq. (7) we solve the kinetic equation for ρ:

$$\frac{\partial\rho}{\partial t} = R_1(I)(\rho_{nt} - \rho) + R_2(I)\rho, \tag{8}$$

where $\rho_{nt} = 5 \times 10^{28}$ $1/\text{m}^3$ is the concentration of neutral atoms in silicon, with $R_1 = \sigma_K I^K$ and $R_2 = \sigma(\omega_0)I/U_i$ being the optical field and avalanche ionization rates, where $I = n_0\varepsilon_0 c_0|E|^2/2$ is the pulse intensity, σ_K is the cross section of the multiphoton ionization, or $\beta_K = K\hbar\omega_0\sigma_K\rho_{nt} = 0.8 \times 10^{-11}$ m/W is the cross section of the multiphoton absorption (adjusted within a range of reported values [17,19] to better fit the measurements), $\sigma(\omega_0) = (2q_e^2/m_e n_0\varepsilon_0 c_0)[\nu_c/(\nu_c^2 + \omega_0^2)]$ is the inverse Bremsstrahlung cross section, and $U_i = 1.12$ eV is the band gap of silicon. To calculate $\partial\rho/\partial t$ in the expression for $\hat{J}_a$ we use only the first term on the right-hand side of Eq. (8). For the refractive index $n(\omega)$ of silicon we use Eq. (22) from Ref. [20] with temperature equal to 293 K.

As initial condition for Eq. (7) we take a flattop beam with the Gaussian temporal profile (similar to our experimental conditions):

$$E(t, x, y, z = 0) = \Theta(a - r)\exp\left[-\frac{(t + dt)^2}{2t_0^2}\right] \times \exp\left(-ik_0\frac{r^2}{2f} - i\omega_0 t\right), \tag{9}$$

where ω_0 is the central frequency, $k_0 = n_0\omega_0/c_0$, and $n_0 = n(\omega_0)$. The spatially dependent temporal delay $dt(r) = n_0 r^2/2fc_0$ in Eq. (9) takes into account that the thickness of the objective lens decreases from the center to the edges. Thus, when a beam passes through the objective its central part becomes delayed relative to its periphery [21]. During the propagation towards the focus, the temporal delay decreases and at the focus all parts of the beam arrive at the same time. For an objective with aperture a, the maximum temporal delay is given by $dt(a) = \text{NA} \times a/2c_0$ [see Eq. (1)]. In the simulations we use the following parameters: $\lambda_0 = 1300$ nm, $t_0 = 60/(2\sqrt{\ln 2})$ fs, $f = 1$ mm, and the objective's aperture a is calculated by Eq. (1) for each specific NA in the experiment. The initial energy of the pulse is 10 nJ, that is, 1 order of magnitude higher than the nonlinear absorption threshold found under similar conditions [22].

In the simulations of ultrashort laser pulses, we need to take into account the dispersion of the refractive index n and for this the corresponding transformation is

$$n_s(\omega) = \frac{n(\omega) - n(\omega_0)}{s} + sn(\omega_0), \tag{10}$$

where ω_0 is the central frequency of the pulse. The first term on the right-hand side of Eq. (10) describes the squeezing of the dispersion curve (which provides the appropriate scaling of the dispersion lengths), and the second one the subsequent scaling. For complex $n(\omega) = n'(\omega) + in''(\omega)$, Eq. (10) should be $n_s(\omega) = \{[n'(\omega) - n'(\omega_0)]/s + sn'(\omega_0)\} + i\{[n''(\omega) - n''(\omega_0)]/s + n''(\omega_0)/s\}$.

In order to apply the transformation approach to Eq. (7), we follow the same procedure as in the previous section, namely, using Eq. (10) with $s = 1000$ we modify the propagation constant k_z and scale up by s times each step along the propagation axis. Note that we need to transform n only in the propagation constant k_z. Any inclusions of the refractive index in the expressions for nonlinear terms must be unchanged in order to preserve the impact of nonlinearities. After this transformation the nonlinear scalar wave equation still describes an equivalent problem, since the length, at which phase and amplitude increments induced by nonlinearities transform the field, is fully determined by the propagation constant k_z.

Figure 4 shows distributions of the fluence, $F(x, z) = \int |E(t, x, y = 0, z)|^2 dt$, measured in the experiment for objectives with different NA and simulated with the transformation approach. As one can see, not only the shape, but also the absolute values of the simulated fluence are very close to the experimental results. As an additional

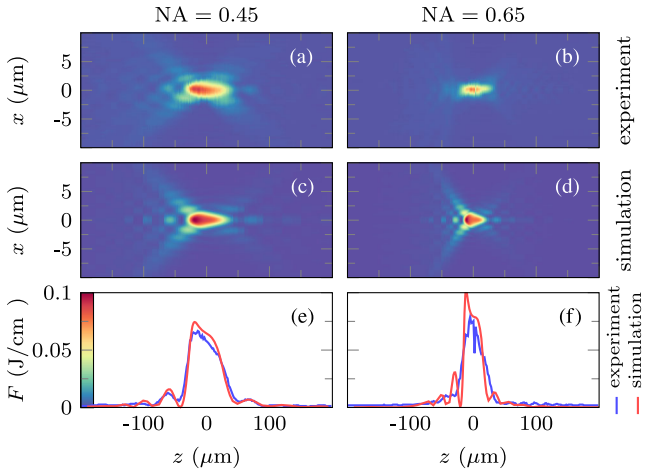

FIG. 4. Fluence distributions of an ultrashort laser pulse focused in silicon by objectives with different NAs. (a),(b) Experiments. (c),(d) Simulations with the transformation approach. (e),(f) Comparison of the on-axis fluences $F(x = 0, z)$. Focal position $f = 1$ mm corresponds to $z = 0$.

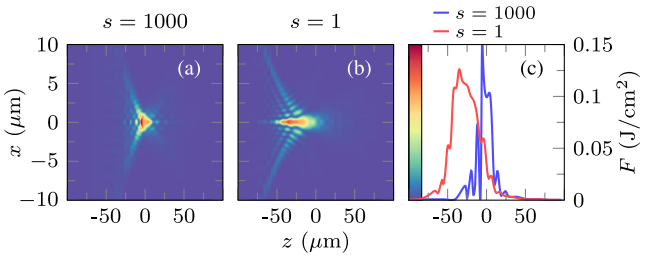

FIG. 5. Simulated fluence distributions of an ultrashort laser pulse focused in silicon by an objective with NA = 1.05, (a) with and (b) without the transformation approach. (c) The corresponding on-axis fluences $F(x = 0, z)$. Focal position $f = 1$ mm corresponds to $z = 0$.

test for the transformation approach we also simulated the above problem in the case of a very low NA (where the propagation is paraxial), first without and then with the transformation, and found no difference in the results (not shown here).

Since the refractive index of silicon is high ($n_0 = 3.51$) the effective values of NA in Fig. 4 are relatively low, so in order to further prove the impact of the transformation approach we separately simulated the same nonlinear problem but with NA = 1.05 that corresponds to NA = 0.3 in vacuum. Figure 5 shows the fluence distributions simulated with and without the transformation. In Fig. 5(b) we see that without the transformation one obtains a fluence distribution that is strongly distorted. Thus, all of the above examples allow us to conclude that with our transformation approach we can accurately simulate the tight focusing of ultrashort laser pulses in nonlinear media.

Conclusions.—In conclusion, we have demonstrated a robust and elegant solution to the problem of simulations of tightly focused ultrashort laser pulses in nonlinear media. Our solution allows one to perform fast simulations of the tight focusing with only scalar wave equations. The original nonparaxial problem is mapped on a problem in a medium with higher refractive index, where the propagation becomes paraxial. This solution can be applied for beams of arbitrary shape and for arbitrary focusing geometries. We demonstrated the validity of our solution both on linear and nonlinear problems against vectorial theory as well as nonlinear propagation experiments and showed that the obtained results are very accurate even in the case of extremely tight focusing. Our solution is expected to enable access to challenging problems of extreme spatiotemporal localization of light energy and their application in different fields, including materials science, plasma physics, and biomedicine, which were until now practically inaccessible.

This work has been performed in the frame of the International Associated Laboratory (LIA) "MINOS" and the QNRF project No. NPRP9-383-1-083.

*v.y.fedorov@gmail.com
†stzortz@iesl.forth.gr

[1] L. Sudrie, A. Couairon, M. Franco, B. Lamouroux, B. Prade, S. Tzortzakis, and A. Mysyrowicz, Phys. Rev. Lett. **89**, 186601 (2002).
[2] R. R. Gattass and E. Mazur, Nat. Photonics **2**, 219 (2008).
[3] A. Vogel, N. Linz, S. Freidank, and G. Paltauf, Phys. Rev. Lett. **100**, 038102 (2008).
[4] M. F. Yanik, H. Cinar, H. N. Cinar, A. D. Chisholm, Y. Jin, and A. Ben-Yakar, Nature (London) **432**, 822 (2004).
[5] A. Vailionis, E. G. Gamaly, V. Mizeikis, W. Yang, A. V. Rode, and S. Juodkazis, Nat. Commun. **2**, 445 (2011).
[6] L. Rapp, B. Haberl, C. J. Pickard, J. E. Bradby, E. G. Gamaly, J. S. Williams, and A. V. Rode, Nat. Commun. **6**, 7555 (2015).
[7] N. M. Bulgakova, V. P. Zhukov, S. V. Sonina, and Y. P. Meshcheryakov, J. Appl. Phys. **118**, 233108 (2015).
[8] S. Chi and Q. Guo, Opt. Lett. **20**, 1598 (1995).
[9] G. Fibich and B. Ilan, Physica (Amsterdam) **157D**, 112 (2001).
[10] C. L. Arnold, A. Heisterkamp, W. Ertmer, and H. Lubatschowski, Opt. Express **15**, 10303 (2007).
[11] P. Jakobsen and J. Moloney, Physica (Amsterdam) **241D**, 1603 (2012).
[12] A. Couairon, O. G. Kosareva, N. A. Panov, D. E. Shipilo, V. A. Andreeva, V. Jukna, and F. Nesa, Opt. Express **23**, 31240 (2015).
[13] M. J. Nasse and J. C. Woehl, J. Opt. Soc. Am. A **27**, 295 (2010).
[14] A. Jarnac, G. Tamosauskas, D. Majus, A. Houard, A. Mysyrowicz, A. Couairon, and A. Dubietis, Phys. Rev. A **89**, 033809 (2014).
[15] C. Xie, V. Jukna, C. Milián, R. Giust, I. Ouadghiri-Idrissi, T. Itina, J. M. Dudley, A. Couairon, and F. Courvoisier, Sci. Rep. **5**, 8914 (2015).
[16] M. Kolesik, J. V. Moloney, and M. Mlejnek, Phys. Rev. Lett. **89**, 283902 (2002).
[17] Q. Lin, J. Zhang, G. Piredda, R. W. Boyd, P. M. Fauchet, and G. P. Agrawal, Appl. Phys. Lett. **91**, 021111 (2007).
[18] A. Mouskeftaras, A. V. Rode, R. Clady, M. Sentis, O. Utéza, and D. Grojo, Appl. Phys. Lett. **105**, 191103 (2014).
[19] A. D. Bristow, N. Rotenberg, and H. M. Van Driel, Appl. Phys. Lett. **90**, 191104 (2007).
[20] H. H. Li, J. Phys. Chem. Ref. Data **9**, 561 (1980).
[21] J.-C. Diels and W. Rudolph, *Ultrashort Laser Pulse Phenomena*, 2nd ed. (Elsevier, New York, 2006), Sec. II.4.
[22] D. Grojo, S. Leyder, P. Delaporte, W. Marine, M. Sentis, and O. Utéza, Phys. Rev. B **88**, 195135 (2013).